

Charge Ordering and Long-Range Interactions in Layered Transition Metal Oxides

Branko P. Stojković,¹ Z. G. Yu,¹ A. R. Bishop,¹ A. H. Castro Neto,² and Niels Grønbech-Jensen¹

¹Theoretical Division and Center for Nonlinear Studies, Los Alamos National Laboratory, Los Alamos, New Mexico 87545

²Department of Physics, University of California, Riverside, California 92521

(Received 28 May 1998)

We study the competition between long-range and short-range interactions among holes within a continuum formulation of the spin density wave picture of layered transition metal oxides. We focus on the problem of charge ordering and the charge phase diagram. The main interactions are the long-range Coulomb interaction and a magnetic dipolar short-range interaction generated by short-range antiferromagnetic fluctuations. Four different phases depending on the strength of the dipolar interaction and the density of holes exist: Wigner crystal, diagonal stripes, horizontal-vertical stripes (loops), and a glassy-clumped phase. The effect of temperature, disorder, and lattice effects on these phases are discussed. [S0031-9007(99)09355-2]

PACS numbers: 71.10.Hf, 71.20.Be

Recently there has been much interest in the charge ordering and domain wall formation at mesoscopic scales in doped transition metal oxides [1]. A popular example of such orderings is stripes, i.e., linear arrays of holes separated by an antiferromagnetically (AF) ordered background. The formation of domain walls and stripes has been discussed in terms of the proximity to phase separation [2]. Macroscopic phase separation has been observed in $\text{La}_2\text{CuO}_{4+\delta}$ [3], and stripes have been observed experimentally in $\text{La}_{2-x}\text{Sr}_x\text{NiO}_{4+y}$ in many different experiments including direct high-resolution electron diffraction [4]. Magnetic susceptibility measurements [5], nuclear quadrupole resonance [6], and muon spin resonance [7] indicate formation of domains in $\text{La}_{2-x}\text{Sr}_x\text{CuO}_4$. Stripes have also been seen in $\text{La}_{1-x}\text{Ca}_x\text{MnO}_3$ for specific commensurate values of doping [8]. A direct evidence for stripe formation was observed in neutron scattering in $\text{La}_{1.6-x}\text{Nd}_{0.4}\text{Sr}_x\text{CuO}_4$ [9]. Moreover, recent neutron scattering experiments are not inconsistent with stripe phases in other high temperature superconductors such as $\text{YBa}_2\text{Cu}_3\text{O}_{7-\delta}$ [10,11].

On the theoretical side, stripes have been proposed as a result of a competition between short-range attractive interaction between holes from the breaking of AF bonds and the long-range Coulomb interaction [12]. Indirect support for this picture has been given in terms of the mapping of the problem into effective spin models [13]. Insulating stripe phases have been obtained within mean field approaches to the short-range Hubbard or t - J models [14]. Numerical methods in these models have not been able to confirm this picture except for recent density matrix renormalization group simulations (DMRG) [15]. *Metallic* stripe phases, proposed to explain experiment [1], have not been obtained theoretically.

In this paper, we present a numerical approach to the problem of holes moving in an AF insulator, in the presence of long-range Coulomb forces, within a continuum approximation. The ability to handle long-range Coulomb interactions at finite density has been enhanced recently in

the area of molecular physics: Assuming a computational cell of arbitrary geometry and cyclic boundary conditions it is possible to sum interactions of particles with all of their images residing in cells obtained by translation from the original computational cell [16,17]. On making integral transformations, Coulomb interactions are computed by summing over fast-convergent Bessel functions with great accuracy.

Using Monte Carlo (MC) and molecular dynamics (MD) methods, we systematically study the interplay between long-range Coulomb interaction and short-range AF interactions of dipolar nature which we take to have both isotropic and anisotropic components (depending on the lattice structure). Our main result is summarized in the phase diagram of Fig. 1. In the absence of disorder, we find four phases depending on the density of holes and the characteristic AF energy scales: a Wigner crystal, diagonal stripes, horizontal-vertical stripes (loops), and a glassy-clumped phase. The striped phases result from the instability of the Wigner crystal, unlike other [12] stripe models. The order parameter for charge ordering is the Fourier transform of the hole density:

$$\rho(\mathbf{q}) = \frac{1}{N} \sum_{i=1}^N e^{i\mathbf{q}\cdot\mathbf{r}_i}, \quad (1)$$

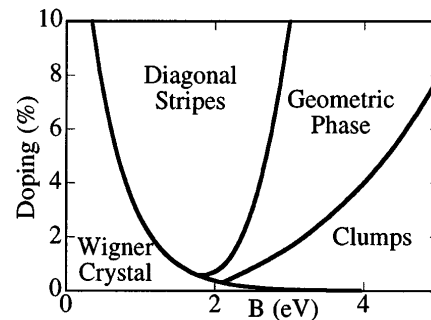


FIG. 1. Phase diagram as a function of the hole density and the strength of the (magnetic) dipolar interaction, B , for $A = 0$.

where \mathbf{r}_i is the position of the i th hole and N is the total number of holes. A peak in $\rho(\mathbf{q})$ at some wave vector $\mathbf{q} = \mathbf{K}$ indicates ordering.

Our starting point is the spin density wave (SDW) picture of the layered transition metal oxides which has been very successful in describing the insulating AF phase of these systems at low temperatures [18,19]. In this picture, the electrons move with hopping energy t in the self-consistent staggered field of its spin. Because the translational symmetry of the system is broken, the electronic band is split into upper and lower Hubbard bands [20]. These are separated by the Mott-Hubbard gap, Δ , and at half filling the lower band is filled and the upper one is empty. This picture is consistent with the angle resolved photoemission data in the layered AF insulator $\text{Sr}_2\text{CuO}_2\text{Cl}_2$ [21]. By doping the system with holes with planar density σ_s and at $T \ll \Delta/k_B$, we focus entirely on the lower band which has a maximum at $\mathbf{k} = \mathbf{Q}/2 = (\pm 1, \pm 1)\pi/2a$, where a is the lattice spacing. It can be shown that the holes interact via two different mechanisms: a short-range attractive and a long-range dipolar interaction [19,22]. The two interactions originate from the AF bond breaking and (dipolar in range) spiral distortions of the AF background [22,23]. The magnetic dipole moment associated with each hole is due to the virtual hopping of holes between neighboring sites and scales with the AF magnetic energy. The magnetic dipolar interaction between two holes with moments $\mathbf{d}_{1,2}$ at distance \mathbf{r} apart has the form

$$U_{\text{dip}} = \frac{1}{r^2} \left[(\mathbf{d}_1 \cdot \mathbf{d}_2) - \frac{2}{r^2} (\mathbf{d}_1 \cdot \mathbf{r})(\mathbf{d}_2 \cdot \mathbf{r}) \right], \quad (2)$$

which is rotationally invariant. It is also possible to show using Ward identities that the spin part of the problem can be described by a two dimensional (2D) nonlinear σ model in the long wavelength limit [24]. At finite T the system is magnetically disordered and characterized by a finite magnetic correlation length, ξ [25], which we introduce phenomenologically [26]. Thus, at finite T the magnetic dipolar interaction between the holes, mediated by the AF background, is actually short ranged. This also reconciles the discrepancy between the vanishing quasi-particle weight Z found for the long-range dipolar interaction and a finite value of Z found in computational studies of the t - J model [26]. However, besides the AF interactions the holes also feel the long-range Coulomb interaction, which we assume is unscreened, as appropriate at low doping where $r_s = r_0/a_0$ (where r_0 is the mean interparticle distance and a_0 is the Bohr radius) is very large ($r_s \approx 8$). Indeed, the interaction energy between the holes, which behaves as $e^2/a_0 r_s$, is certainly more important than the kinetic energy term ($\approx e^2/a_0 r_s^2$) at low densities; hence, the interaction terms should be treated first and the kinetic energy as a perturbation. Finally, each hole carries a spin degree of freedom as well, but it is possible to show that the overall spin energy is minimized in the spin antisymmetric channel, as we as-

sume here. Thus, we are left with only the charge channel with an effective (magnetic in origin) interaction between two holes, 1 and 2, of the form [see Eq. (2)]

$$V(\mathbf{r}) = \frac{q^2}{r} - A e^{-r/a} - B \cos(2\theta - \phi_1 - \phi_2) e^{-r/\xi}, \quad (3)$$

where q is the hole charge, θ is the angle made between \mathbf{r} and a fixed axis, and $\phi_{1,2}$ are the angles of the magnetic dipoles relative to the same fixed axis, which we assume can take an arbitrary value. A is the strength of the short-range anisotropic interaction ($A \approx U$ when $t \gg U$ and $A \approx 4t^2/U$ when $U \gg t$ [23]), and B is the strength of the magnetic dipolar interaction [$B \approx A/(2\pi\xi^2)$], which we will assume to be independent variables. The magnetic correlation length ξ is obtained from neutron scattering measurements [28]: We have assumed $\xi = 3.8/\sqrt{x}$ Å throughout the manuscript; we further discuss ξ dependence of our results below.

In general, the many-body problem of holes in an AF background is extremely complicated, involving many-particle interaction terms. However, at low densities it is reasonable to assume that the interaction of any two holes is weakly perturbed by other holes, and the total potential energy can be expressed in terms of two-particle energies [29]. Therefore, in our numerical calculations we study the physics of N holes interacting via $V(\mathbf{r})$ as given in (3). We assume a rectangular computational box of size $L_x \times L_y$ with L_x, L_y up to 100 unit cells in a CuO_2 plane. At the beginning of each simulation, we place the holes at random and assign to each hole a magnetic dipole moment of constant size, but random direction. We find a minimum of the total potential in this system using three different methods: MC method, Langevin MD, and a hybrid MC-MD method [30]. In order to rapidly reach a hole configuration with the lowest global minimum energy, we perform simulated annealing from high temperatures. All three methods yield essentially the same results.

For $B = 0$ we find the Wigner crystal with small distortions [31] to be the state of lowest energy, as expected [32]. Increasing A while retaining $B = 0$ reduces the lattice constant of the Wigner crystal until a critical value is reached where holes group together. For $A = 0$ and finite B the situation is quite different. At small B and larger densities the Wigner crystal is unstable and a new phase with diagonal stripes is formed [33]. This phase is characterized by ferrodipolar order (see Fig. 2a). The situation here is very similar to that observed in $\text{La}_{2-x}\text{Sr}_x\text{NiO}_{4+y}$ [4]. As shown in Fig. 2c, at larger values of B a line stripe is formed, which, with increasing density, tends to close into loops, forming a checkerboard pattern. Importantly, the loop formation is accompanied by magnetic dipole orientation along the straight portion of a loop with gradual rotation by $\pi/2$ at each corner [34]. Because of the rotation of dipoles at the corners, the loops interact and eventually form the checkerboard pattern [35]. The size of the interhole distance within a line is determined

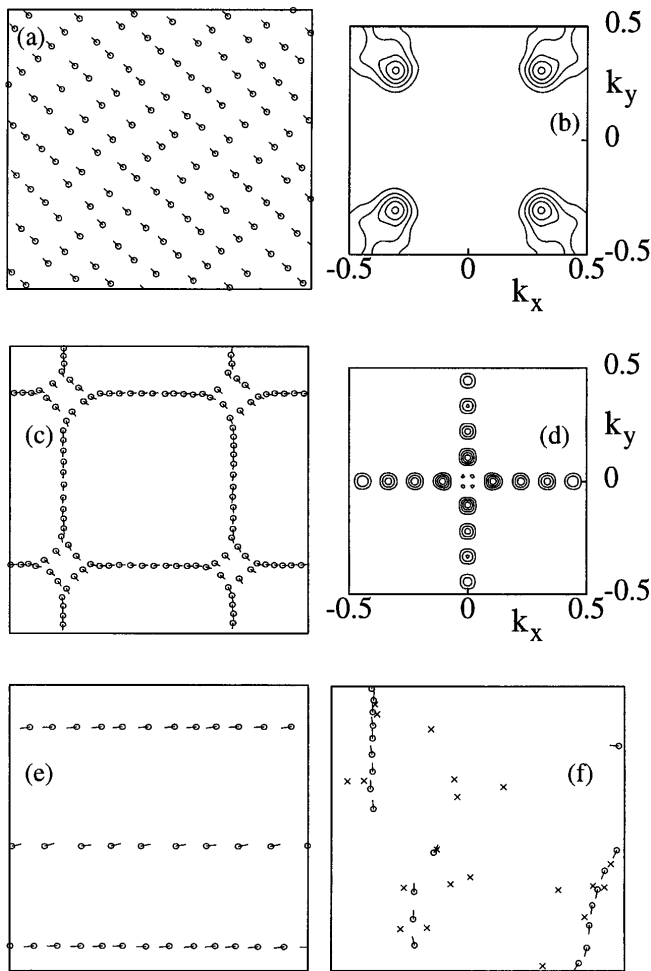


FIG. 2. Geometric phases resulting from the competition of magnetic dipolar and Coulomb interactions: Panels (a) and (c) show holes (open circles) with their dipole orientations, in a small section of the computational box, for the ferrodipolar and stripe phases, respectively; panels (b) and (d) show contour plots of the hole density in momentum space [see Eq. (1)] for the phases shown in panels (a) and (c). Panel (e) shows the stripe phase obtained with magnetic dipole anisotropy of 0.8, and panel (f) hole positions in the presence of impurities (crosses).

by the ratio of B and the Coulomb energy; the loop sizes are determined by the hole density alone. These results appear to be consistent with the DMRG solution of the t - J model [15]. If B is increased further, the magnetic dipolar interaction becomes dominant over the average Coulomb interaction; the well-defined pattern disappears and one observes star shaped clumps of holes, which can, at sufficiently high density, form another geometric structure (e.g., a Wigner crystal of clumps). We remark that assuming a larger value of ξ or a screened Coulomb potential with a dielectric constant ~ 10 leads to a decrease in the effective value of B at which the transitions occur (Fig. 1). The same occurs on using a nonvanishing value of A ; however, the isotropic term A alone (in the absence of crystal symmetry effects) *never* produces any nontrivial geometric phase (e.g., stripes). We find that the transition

between the ferrodipolar and the stripe phase is first order, while other transitions appear to be of second order [31].

In the cases presented above, we have assumed uniform magnetic dipolar interaction. It is well known that there are orthorhombic and tetragonal distortions in practically all transition metal oxides. In particular, static stripe formation has been observed only in the low temperature tetragonal phase of $\text{La}_{1.6-x}\text{Nd}_{0.4}\text{Sr}_x\text{CuO}_4$ [9]. In order to study the influence of the anisotropy, we assume that the magnetic dipole sizes along x and y directions have anisotropy α ($\alpha = 1$ corresponds to the isotropic case). Figure 2e shows our solution for $\alpha = 0.8$: The symmetry is broken and a stripe superlattice is formed, with a charge ordering vector $\mathbf{K} = (\pi/\ell)\mathbf{x}$, where 2ℓ is the interstripe distance. In the SDW model, the Fourier transform of the magnetization $S(\mathbf{q}) = \langle S_z(\mathbf{q}) \rangle$ is slaved to (1) such that a peak at \mathbf{K} in (1) leads to a peak at $\mathbf{Q} \pm \mathbf{K}/2$ in $S(\mathbf{q})$ [31]. Thus, our results yield a neutron peak at $(\pi/a \pm \pi/2\ell, \pi/a)$. Assuming twinning, this would imply neutron peaks at $(\pi/a \pm \pi/2\ell, \pi/a \pm \pi/2\ell)$ in agreement with experiment [11]. The same is obtained in the checkerboard phase (see Figs. 2c and 2d). If one includes the kinetic energy [31], instead of static stripe formation one would obtain dynamical stripes such as those believed to exist in $\text{La}_2\text{Sr}_x\text{CuO}_4$. In this case, the Fermi surface of the system should be modified by the superlattice formation [36]. The kinetic energy may also destroy the ferrodipolar phase and certainly the Wigner crystal phase, even at relatively low temperatures [31].

It should be noted that the shift from \mathbf{Q} of $S_z(\mathbf{q})$, due to hole ordering, alters the effective interaction [Eq. (3)] which, in turn, changes the position of the peak in S_z ; the final solution should be obtained self-consistently. Our results are also somewhat sensitive to the applied boundary conditions: First, the exact size of the checkerboards depends on its commensuration with the computational box, which, in turn depends on the density. On increasing of the size of the computational box, the checkerboard pattern shown in Fig. 2c acquires point or line defects [31]. This leads to the reduction in the higher order peaks observed in Fig. 2d with no change in their wave numbers. Second, in a finite system with appropriate charge background, the holes do not form geometric phases, although they still form stripes [31]. However, in this case, even a very small anisotropy ($\alpha \sim 0.95$) again leads to stripe formation as in Fig. 2e [31].

We have also studied impurity effects (from defects or charged counterions). For example, we place the same number of impurities as holes, randomly in a plane a distance $d = 6 \text{ \AA}$ above the plane to simulate the situation in, e.g., Sr doped cuprates and consider the *unscreened* attractive Coulomb interaction between impurity and hole. The charge pattern produced is very sensitive to impurity doping (see Fig. 2f). The Wigner crystal becomes glassy with no obvious sign of charge ordering. This happens because the attractive Coulomb energy between impurities and holes scales as e^2/d

while the average interhole Coulomb energy behaves as $e^2\sqrt{\sigma_s}$. Thus, when $\sigma_s < 1/d^2$ the holes are pinned by impurities. Most strikingly, all other phases are unstable towards *finite* stripe formation. The loops and diagonal stripes tend to deform to pass very close to the impurities in order to maximize the attractive energy. However, the magnetic dipole interaction is sufficient to retain the main orientation. This leads us to conjecture that with the addition of the kinetic energy the holes can move in string segments in an orientation given basically by the phase diagram of the clean system. These string segments are kept together by the dipolar interaction (i.e., string tension). The stripe motion would then be caused by mesoscopic thermal or quantum tunneling of the finite strings between the minima of the overall potential. This would lead to nonlinear effects in the low temperature field dependent conductivity [37] and unusual T dependence of the conductivity [31]. We have also performed simulations in the presence of a realistic underlying periodic lattice and have found that this creates slight distortions in the phases, pinning loops more strongly [31]. In particular, the peaks in $\rho(\mathbf{q})$ sharpen in some of these phases. Finally, at finite T melting of the phases occurs because of the small energy scales and large entropy in long-range Coulomb tails.

In summary, using a novel numerical technique, we have studied the competition between long-range and short-range interactions and its impact on hole ordering in layered transition metal oxides. Employing the SDW picture of these systems, we have studied the short-range attractive force and the dipolar force generated by the short-range AF fluctuations together with long-range Coulomb forces for a 2D layer. We have found a rich phase diagram for the clean system which includes a Wigner solid, stripes, loops, and a glassy phase. This phase diagram is consistent with several different experimental measurements. We have also found this system to be rather sensitive to the presence of charged impurities. However, the stripe phases survive as finite stripe segments which we believe is key to understanding these systems. We remark that the stripes observed in our study are insulating; the stability of the proposed metallic stripe phases remains an open and puzzling problem.

We gratefully acknowledge valuable discussions with A. Balatsky, A. Chernyshev, J. Gubernatis, C. Hammel, S. Kivelson, D. Pines, D. Scalapino, J. Schmalian, S. White, and J. Zaanen. A.H.C.N. acknowledges support from the Alfred P. Sloan foundation. Work at Los Alamos was supported by the U.S. Department of Energy. Work at the University of California, Riverside, was partially supported by a Los Alamos CULAR project.

[1] J.M. Tranquada, *J. Phys. Chem. Solids* **59**, 2150 (1998).

[2] *Phase Separation in Cuprate Superconductors*, edited by K.A. Müller and G. Benedek (World Scientific, Singapore, 1993).

- [3] P.C. Hammel *et al.*, in Proceedings of the Conference on Anharmonic Properties of High Tc Cuprates, 1994.
- [4] J.M. Tranquada *et al.*, *Phys. Rev. Lett.* **70**, 445 (1993).
- [5] J.H. Cho *et al.*, *Phys. Rev. Lett.* **70**, 222 (1993).
- [6] F.C. Chou *et al.*, *Phys. Rev. Lett.* **71**, 2323 (1993).
- [7] F. Borsa *et al.*, *Phys. Rev. B* **52**, 7334 (1995).
- [8] S. Mori *et al.*, *Nature (London)* **392**, 473 (1998).
- [9] J.M. Tranquada *et al.*, *Nature (London)* **375**, 561 (1995).
- [10] J.M. Tranquada *et al.*, *Physica (Amsterdam)* **282**, 166 (1997).
- [11] G. Aeppli *et al.*, *Science* **278**, 1432 (1997).
- [12] V.J. Emery and S.A. Kivelson, *Physica (Amsterdam)* **209C**, 597 (1993).
- [13] U. Löw *et al.*, *Phys. Rev. Lett.* **72**, 1918 (1994); S. Haas *et al.*, *Phys. Rev. B* **51**, 5989 (1995).
- [14] H.J. Schulz, *J. Phys. (Paris)* **50**, 2833 (1989); J. Zaanen and J. Gunnarsson, *Phys. Rev. B* **40**, 7391 (1989); A.R. Bishop *et al.*, *Europhys. Lett.* **14**, 157 (1991).
- [15] S.R. White and D.J. Scalapino, *Phys. Rev. Lett.* **80**, 1272 (1998).
- [16] J. Lekner, *Physica (Amsterdam)* **176A**, 485 (1991).
- [17] N. Grønbech-Jensen *et al.*, *Mol. Phys.* **92**, 941 (1997).
- [18] J.C. Slater, *Phys. Rev.* **82**, 538 (1951).
- [19] J.R. Schrieffer, X.G. Wen, and S.C. Zhang, *Phys. Rev. B* **39**, 11 663 (1989).
- [20] N.F. Mott, in *Metal-Insulator Transitions* (Taylor & Francis, London, 1974), p. 141.
- [21] B.O. Wells *et al.*, *Phys. Rev. Lett.* **74**, 964 (1995).
- [22] B.I. Shraiman and E.D. Siggia, *Phys. Rev. B* **40**, 9162 (1989).
- [23] D.M. Frenkel and W. Hanke, *Phys. Rev. B* **42**, 6711 (1990).
- [24] E. Fradkin, in *Field Theories of Condensed Matter Systems* (Addison-Wesley, Redwood City, CA, 1991), p. 48.
- [25] S. Chakravarty *et al.*, *Phys. Rev. Lett.* **60**, 1057 (1988).
- [26] It has been found, both numerically and analytically, that the long-range spiral ordering may be unstable even at $T = 0$ (see, e.g., Ref. [27] and A. Auerbach, in *Interacting Electrons and Quantum Magnetism* (Springer-Verlag, New York, 1994).
- [27] For a discussion, see, e.g., E. Dagotto, *Rev. Mod. Phys.* **66**, 763 (1994).
- [28] R.J. Birgeneau *et al.*, *Phys. Rev. B* **38**, 6614 (1988).
- [29] T. Dombre, *J. Phys. (Paris)* **51**, 847 (1990).
- [30] J. Bonča and J.E. Gubernatis, *Phys. Rev. E* **53**, 6504 (1996).
- [31] Details of this calculation will be given elsewhere.
- [32] E.P. Wigner, *Phys. Rev.* **46**, 1002 (1934).
- [33] A phase similar to this one has been proposed in Ref. [29].
- [34] This is a highly degenerate configuration which can be mapped into a classical six vertex model [31]. See, e.g., R.J. Baxter, in *Exactly Solved Models in Statistical Mechanics* (Academic Press, London, 1982), p. 127.
- [35] The simulations show the presence of topological defects in the phase of the magnetic dipole moments, i.e., the total phase in a loop may be shifted by 2π .
- [36] A.H. Castro Neto and F. Guinea, *Phys. Rev. Lett.* **80**, 4040 (1998).
- [37] J. Bardeen, *Phys. Rev. Lett.* **45**, 1978 (1980); D.S. Fisher, *Phys. Rev. B* **31**, 1396 (1985).